AN ARCHITECTURE FOR ACTIVE METAMATERIAL PARTICLES AND EXPERIMENTAL VALIDATION AT RF

Bogdan-Ioan Popa and Steven A. Cummer
Department of Electrical and Computer Engineering, Duke University, Durham, NC 27708; Corresponding author: bap7@ee.duke.edu

Received 21 March 2007

ABSTRACT: *We describe a class of metamaterial particle that employs active elements to overcome the inherent limitations of their passive counterparts, such as significant losses, high dispersion, and narrow bandwidth. The active unit cell can be designed to have either an electric or magnetic response. For a magnetic active metamaterial, we derive the design equations for the unit cell and validate them experimentally through the extraction of effective permittivity and permeability from* S*-parameter measurements of a unit cell in a waveguide. We show that phase delay in the amplifier can be used to control losses and dispersion.* © 2007 Wiley Periodicals, Inc. Microwave Opt Technol Lett 49: 2574–2577, 2007; Published online in Wiley InterScience (www.interscience.wiley.com). DOI 10.1002/mop.22789

Key words: *active metamaterials; magnetic active metamaterials*

1. INTRODUCTION

Engineered electromagnetic materials, or metamaterials, have properties that could potentially be used to fabricate super lenses [1], miniaturized antennas [2], enhanced tunneling effect devices [3], or even invisibility cloaks [4, 5]. Electric and magnetic metamaterials have been extensively analyzed theoretically, in simulations, and tested experimentally, and are currently built by putting together arrays of passive subwavelength resonant particles, such as split-ring-resonators (SRRs) [6, 7], omega particles [8], electric-field-coupled resonators (ELCs) [9], or cut-wires [10, 11].

The currents and charges in these passive, self-resonant circuits created in response to an applied electric or magnetic field are big enough near the resonant frequency to generate electric or magnetic dipole moments that are in turn big enough to substantially alter the effective permittivity or permeability of a medium composed of these particles. However, exploiting this strong response close to resonance usually means significant losses and strongly frequency-dependent properties, two properties undesirable in many potential metamaterial applications. For example, it has been shown both theoretically [12] and experimentally [13] that the smallest amount of loss could significantly influence the effectiveness of the evanescent wave enhancement property responsible for the super lens and enhanced tunneling effects. On the other hand, it has been shown that even modest loss tangents of 0.01 can rarely be achieved in these metamaterials [14]. Also, because of their resonant nature, the inherent high dispersion makes them useful only for narrow bandwidth applications.

2. METHOD AND RESULTS

It has long been recognized [15] that metamaterials containing active elements can in principle be used to reduce or control with greater flexibility these limitations on loss and dispersion. Microwave amplifiers, together with the transmission line equivalent of left-handed materials, have already been shown to improve the characteristics of leaky-wave antennas [16]. In principle, metamaterial particles that employ active gain elements can generate similarly strong material responses without relying on resonances and can thus provide the ability to control losses and dispersion. We propose the general approach illustrated in Figure 1 to create active metamaterial particles. The idea behind the active particle is to use a sensing element to generate a voltage proportional to the external field. For a magnetic particle, this element could be a loop, whereas for an electric particle this element could be a short wire. This sensed voltage is amplified by an amplifier which, in turn, drives the driven element that produces an electric or magnetic dipole moment. This architecture could also be used to create active cross-polarizing elements by rotating the driven loop relative to the sensing loop and also magnetoelectric elements by mixing electric sensing loops and magnetic driven loops or vice versa.

Our goal is to derive the design equations for such an active unit cell and verify their validity experimentally, thereby confirming that this class of unit cell can be used to create an active metamaterial. We will also see how losses and dispersion can be controlled through the phase delay of the gain element. We will focus here on developing magnetic active particles capable of generating non-unity metamaterials. However, as shown in Figure 1, the principles discussed in this article can also be applied to obtain electric metamaterials.

To begin our analysis, we consider a plane wave propagating in free space. For the purpose of this article, the magnetic unit cell shown in Figure 1 is positioned such that the sensing and driven loops are parallel to each other and are both perpendicular on the external magnetic field. This makes the material anisotropic with a non-unity component on the diagonal of the permeability tensor in the direction perpendicular to the loops. The equivalent circuit of this active unit cell is given in Figure 2.

To control the phase delay through the system, we connect the sensing and driven loops to the amplifier through transmission lines of characteristic impedance Z_0, and lengths l_1 and l_2, respectively. The amplifier has input impedance Z_{in}, output impedance Z_{out}, and gain G. The voltage picked up by the sensing loop of area A_{i} and inductance L_{i} satisfies the equation

$$\nu_{\text{in}} = -j\omega\mu_0 H A_{\text{i}}, \tag{1}$$

where H is the externally applied magnetic field, and we require the loop to be much smaller than the wavelength. Note that in the previous equation we neglect the magnetic coupling between the driven and sensing loops; however this is justified by the experimental data. Given these parameters it is straightforward to show that, assuming no magnetic coupling between the two loops, the voltage ν_{out} across the driven loop of area A_{o} and inductance $L_{\text{o}}$is given by

$$\nu_{\text{out}} = \nu_{\text{in}} G \frac{Z_0}{Z_0 + j\omega L_{\text{i}}} \times \frac{1+\Gamma_{\text{in}}}{e^{j\beta_1 l_1} - \Gamma_{\text{in}}\Gamma'_{\text{in}} e^{-j\beta_1 l_1}} \frac{Z_0}{Z_0 + Z_{\text{out}}} \frac{1+\Gamma_{\text{out}}}{e^{j\beta_2 l_2} - \Gamma_{\text{out}}\Gamma'_{\text{out}} e^{-j\beta_2 l_2}}, \tag{2}$$

where β_1 and β_2 are the propagation constants through the two transmission lines and

$$\Gamma_{\text{in}} = \frac{Z_{\text{in}} - Z_0}{Z_{\text{in}} + Z_0}; \quad \Gamma'_{\text{in}} = \frac{j\omega L_{\text{i}} - Z_0}{j\omega L_{\text{i}} + Z_0}, \tag{3}$$

$$\Gamma_{\text{out}} = \frac{j\omega L_{\text{o}} - Z_0}{j\omega L_{\text{o}} + Z_0}; \quad \Gamma'_{\text{out}} = \frac{Z_{\text{out}} - Z_0}{Z_{\text{out}} + Z_0}. \tag{4}$$

From these equations it follows that the currents through the sensing and driven loops are $i_{\text{in}} = \nu_{\text{in}}/j\omega L_{\text{i}}$ and, respectively, $i_{\text{out}} = \nu_{\text{out}}/j\omega L_{\text{o}}$. Therefore, the magnetic moment generated in this unit cell is $m = i_{\text{in}}A_{\text{i}} + i_{\text{out}}A_{\text{o}}$, and assuming that the unit cell has

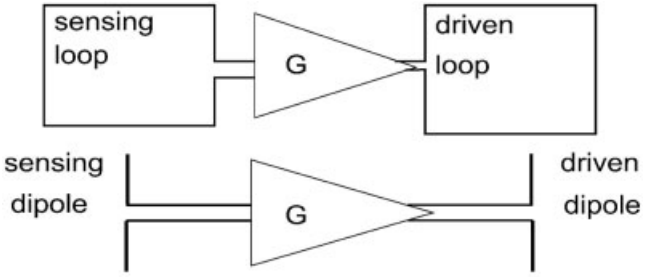

Figure 1 Concept of the active magnetic (top) and electric (bottom) cell

volume V_{uc} it follows that the effective relative permeability of a metamaterial made of arrays of such cells is

$$\mu_r = 1 + \frac{m}{HV_{uc}} = 1 - \frac{\mu_0 A_i}{V_{uc}}\left(\frac{A_i}{L_i} + \frac{A_o}{L_o} G_{eff}\right), \quad (5)$$

where G_{eff} is the equivalent gain of the system defined as $G_{eff} = \nu_{out}/\nu_{in}$.

Equations (2)–(5) are the design equations for the unit cell depicted in Figure 1. In the following discussion, μ_r' and μ_r'' are the real and imaginary parts of μ_r. If we require zero losses in a metamaterial made of such unit cells, we need $\mu_r'' = 0$, which means, from Eq. (5), that G_{eff} has to be real, or, equivalently, ν_{out} and ν_{in} have to be either in phase or 180° out of phase. A closer look to Eq. (2) reveals that this occurs periodically in frequency because ν_{out} varies periodically with frequency because of the delay in the transmission lines and the phase distortions of the amplifier. Moreover, if the amplitude $|G|$ is approximately constant with frequency in the band of interest, as is true for most amplifiers, then the amplitude $|\nu_{out}|$ varies slowly with frequency, which means that μ_r' oscillates around 1 with minima and maxima at frequencies where, again, ν_{out} and ν_{in} are in phase or 180° out of phase, and where $\mu_r'' \approx 0$. We wish to show this feature in the following experiments.

We used a microstrip transmission line to excite TEM modes below 900 MHz inside it. Two circular metallic loops of radius 1.8 cm oriented parallel to each other and the axis of the microstrip are placed inside the waveguide as illustrated in Figure 3. The distance between them was 6 cm. SMA cables 1 m long entering the microstrip through two holes drilled through the waveguide walls were used to connect the two loops to an AR 1W1000 microwave amplifier placed outside the waveguide. The amplifier has a 30 ± 1.5 dB gain between 1 MHz and 1 GHz, 50 Ω input and output impedances, has linear phase distortions, and can drive purely inductive loads. Since we are interested in frequencies below 900 MHz, the sensing and driven loops are λ/8 or smaller, and the

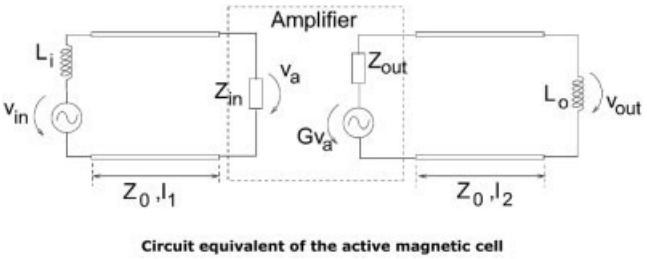

Figure 2 Circuit equivalent of the active magnetic cell

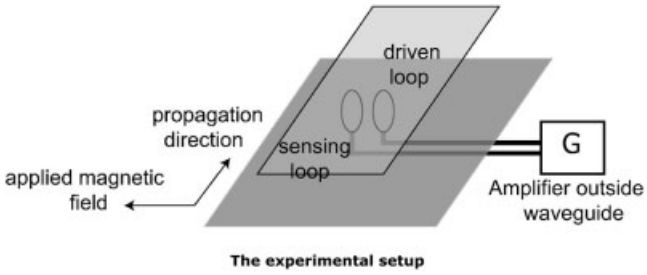

Figure 3 The experimental setup

effective medium approximation assumed here holds. We used an Agilent 8720A network analyzer to measure the reflected and transmitted waves through the waveguide. We have a single sensing/driven loop configuration, and so we can consider that we have only one unit cell filling the transverse section of the waveguide. Under these assumptions, we use the procedure described in Ref. 17 to retrieve the effective permeability of such a medium. The result is plotted in Figure 4 (the solid lines).

The permeability follows closely the expected theoretical predictions (the dotted lines), which validates Eqs. (1)–(5). Moreover, we notice the important features expected theoretically, namely, μ_r' oscillates around 1, with maxima and minima occurring at frequencies where μ_r' is approximately zero. Thus, for example, at around 602 MHz the dispersion is almost zero ($d\mu_r'/d\omega \approx 0$) as well as the loss ($\mu_r'' \approx 0$). Notice that, according to the design equations, in the regions where the amplifier is linear, the response of the active cell is also linear; therefore, the Kramers–Kronig relations must apply. As a result, at the frequencies where we have anomalous dispersion (i.e. $d\mu_r'/d\omega < 0$) we must have either loss or gain, which is in agreement with the retrieved permeability.

To make sure that the good match between the theoretical and experimentally retrieved permeability is not a coincidence, we repeated the experiment with a different amplifier. We replaced the AR 1W1000 amplifier with a Minicircuits ZHL2010 microwave amplifier in series with a Maxim MAX2472 voltage buffer. The gain of this system was, again, ~30 dB. The output impedance given in the datasheets and measured with the network analyzer was $(91 - j182)$ Ω, and was slowly varying with frequency; thus

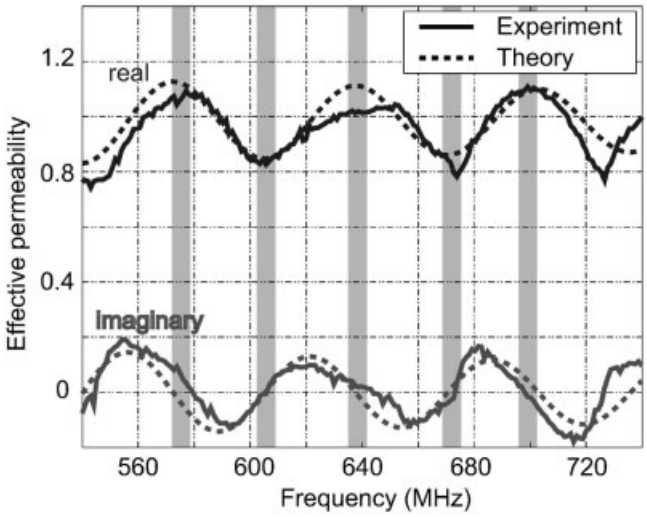

Figure 4 Effective permeability retrieved from measurements for a unit cell containing an 1W1000 amplifier. There are frequencies with almost no dispersion and zero loss (the shadowed regions)

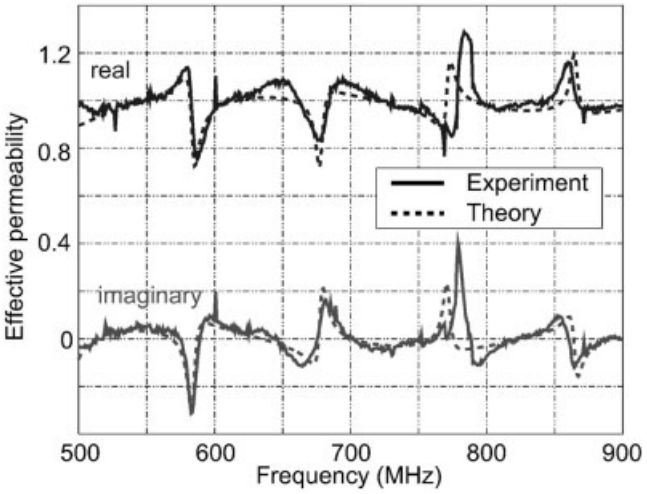

Figure 5 Match between the theoretical and retrieved permeability for a unit cell containing the minicircuits ZHL2010 amplifier connected to the Maxim MAX2472 voltage buffer

we approximated it as being constant throughout the frequency band of interest. We expected the capacitive component of this impedance together with the inductance of the driven loop to create resonant features in the retrieved permeability. Moreover, we expected these features to be periodic because of the linear phase distortions of the amplifier and buffer, and the length of the cables, as discussed above. Indeed, the experimentally retrieved permeability presented in Figure 5 clearly shows these features. Moreover, the good agreement between the experiment and the theoretical predictions in this much more complicated case further verify the validity of Eqs. (2)–(5).

These equations allow us to easily design a unit cell that could be used to generate a metamaterial having negative effective permeability. Thus, assuming that the sensing and driven loops are kept unchanged, to increase the magnetic moment generated in response to an applied magnetic field, it follows from Eq. (5) that we have to either increase the concentration of unit cells by decreasing V_{uc} or increase v_{out}. From Eq. (2) the latter can be achieved by increasing the amplifier gain, G, its input impedance, Z_{in}, or by decreasing the output impedance, Z_{out}. Thus, assuming a unit cell occupying a volume three times smaller than in the previous experiments, and a miniature amplifier placed inside the cell next to the two loops and having a gain of 40 dB; 200 Ω, input impedance; 50 Ω, output impedance; and same linear phase distortions as AR 1W1000, it follows from Eq. (5) that we can achieve the relative permeability illustrated in Figure 6. Notice that the oscillatory behavior in this case is caused only by the phase distortions of the amplifier, which explains the bigger period. It follows from Eqs. (2) and (5) that the frequency at which zero losses and essentially no dispersion is achieved can be tuned by changing the phase delay through the amplifier (i.e. the phase of G) to bring v_{out} and v_{in} in phase at the desired frequency.

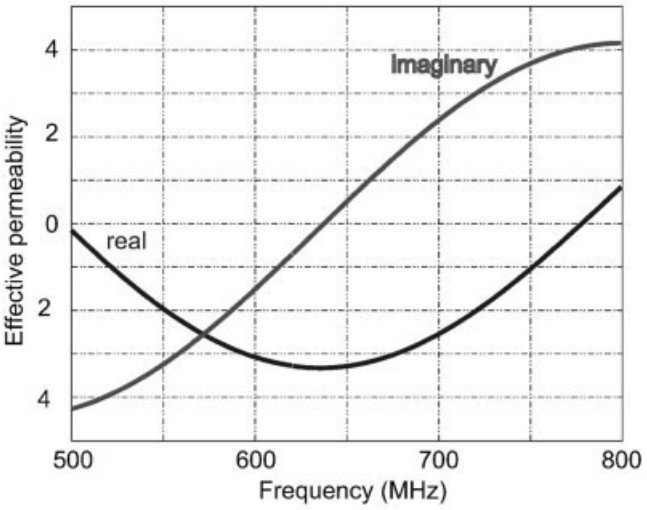

Figure 6 Theoretically achievable effective permeability in a metamaterial composed of active unit cells, provided the right amplifier is used

3. CONCLUSION

In conclusion, we described an architecture for active metamaterial unit cells that employs a field sensing element, an amplifier, and a driven element that produces the electric or magnetic dipole moment material response. Full design equations for the specific case of an active magnetic metamaterial were derived and validated through single unit cell experimental measurements. This active magnetic metamaterial exhibits dispersion and loss characteristics that are dramatically different from those found in passive resonant metamaterials, including frequencies where the permeability is less than unity yet with zero loss and near zero dispersion. By controlling the amplifier characteristics, most importantly the phase, a very wide set of metamaterial characteristics can be achieved through this active cell approach.

REFERENCES

1. J.B. Pendry, Negative refraction makes perfect lens, Phys Rev Lett 85 (2000), 3966–3969.
2. R.W. Ziolkowski and A.D. Kipple, Application of double negative materials to increase the power radiated by electrically small antennas, IEEE Trans Antennas Propag 51 (2003), 2626–2640.
3. J.D. Baena, L. Jelinek, R. Marques, and F. Medina, Near-perfect tunneling and amplification of evanescent electromagnetic waves in a waveguide filled by a metamaterial, Phys Rev B 72 (2005), 075116.
4. J.B. Pendry, D. Schurig, and D.R. Smith, Controlling electromagnetic fields, Science (2006), 1780–1782.
5. S.A. Cummer, B.-I. Popa, D.S. Schurig, D.R. Smith, and J. Pendry, Full-wave simulations of electromagnetic cloaking structures, Phys Rev E 74 (2006), 036621.
6. J.B. Pendry, A.J. Holden, D.J. Robbins, and W.J. Stewart, Magnetism from conductors and enhanced nonlinear phenomena, IEEE Trans Microwave Theory Tech 47 (1999), 2075–2084.
7. D.R. Smith, W.J. Padilla, D.C. Vier, S.C. Nemat-Nasser, and S. Schultz, Composite medium with simultaneously negative permeability and permittivity, Phys Rev Lett 84 (2000), 4184–4187.
8. L. Ran, J. Huangfu, H. Chen, Y. Li, X. Zhang, K. Chen, and J.A. Kong, Microwave solid-state left-handed material with a broad bandwidth and an ultralow loss, Phys Rev B 70 (2004), 073102.
9. D. Schurig, J.J. Mock, and D.R. Smith, Electric-field-coupled resonators for negative permittivity metamaterials, Appl Phys Lett 88 (2006), 041109.
10. J.B. Pendry, A.J. Holden, W.J. Stewart, and I. Youngs, Extremely low frequency plasmons in metallic mesostructures, Phys Rev Lett 76 (1996), 4773–4776.
11. D.R. Smith, D.C. Vier, W. Padilla, S.C. Nemat-Nasser, and S. Schultz, Loop-wire medium for investigating plasmons at microwave frequencies, Appl Phys Lett 75 (1999), 1425–1427.
12. D.R. Smith, D. Schurig, M. Rosenbluth, S. Schultz, S. A. Ramakrishna, and J.B. Pendry, Limitations on subdiffraction imaging with a negative refractive index slab, Appl Phys Lett 82 (2003), 1506–1508.
13. B.-I. Popa and S.A. Cummer, Direct measurement of evanescent wave

enhancement inside passive metamaterials, Phys Rev E 73 (2006), 016617.
14. S.A. Cummer, B.-I. Popa, and T. Hand, p. arXiv:physics/0703130 (2007).
15. S.A. Tretyakov, Meta-materials with wideband negative permittivity and permeability, Microwave Opt Technol Lett 31 (2001), 163–165.
16. F.P. Casares-Miranda, C. Camacho-Penalosa, and C. Caloz, High-gain active composite right/left-handed leaky-wave antenna, IEEE Trans Antennas Propag 54 (2006), 2292–2300.
17. D.R. Smith, S. Schultz, P. Markos, and C.M. Soukoulis, Determination of effective permittivity and permeability of metamaterials from reflection and transmission coefficients, Phys Rev B 65 (2002), 195104.

FRACTAL-SHAPED HI-LO MICROSTRIP LOW-PASS FILTERS WITH HIGH PASSBAND PERFORMANCE

Wen-Ling Chen,[1] Guang-Ming Wang,[1] and Yi-Na Qi[2]
[1] Radar Engineering Department, Missile Institute of Air Force Engineering University, Sanyuan, Shaanxi 713800, China, Corresponding author: wlchen_2003@yahoo.com.cn
[2] Computer Engineering Department, Missile Institute of Air Force Engineering University, Sanyuan, Shaanxi 713800, China

Received 27 March 2007

ABSTRACT: *Hi-Lo microstrip low-pass filters using Koch fractal shapes are proposed for the first time. By constructing the low-impedance sections in Koch-shaped geometry, the passband performance of the Hi-Lo microstrip low-pass filter enhanced greatly. The excellent passband performance is mainly due to the gradual changes of the steps of the fractal-shaped microstripline, thus to provide weak current discontinuities. To verify the proposed method, low-pass filter prototypes of different iteration orders are designed, fabricated, and measured, and the measurement results show that the maximal sidelobe level of the passband return loss is reduced from −17.8 to −28.6 dB, and the other performances are not changed.* © 2007 Wiley Periodicals, Inc.
Microwave Opt Technol Lett 49: 2577–2579, 2007; Published online in Wiley InterScience (www.interscience.wiley.com). DOI 10.1002/mop.22774

Key words: *fractal-shape; hi-lo microstripline; low-pass filter (LPF)*

1. INTRODUCTION

A compact and high performance microwave low-pass filter is highly desirable in wireless communication systems, such as satellite and mobile communication systems, to suppress harmonics. One of the conventional filters is the Hi-Lo microstrip filter mainly due to the ease of implementation in either microstrip or coplanar technology. The filter is normally composed of alternating low and high impedance regions where the change in impedance is controlled by the line width of the strip. For achieving a high degree of attenuation in the stopband, it is necessary to increase the order of the filter or obtain a big high to low impedance ratio (Z_h/Z_1) [1, 2]. However, if the filter order is increased, the size of the entire circuit will be incremented, and if the impedance ratio is big enough, the passband performance will be degraded because of sharp current discontinuities in the steps. To enhance the passband performance for a LPF with big impedance ratio, electromagnetic bandgap (EBG) structures are used [3], however, since the frequency selective properties of EBGs are based on the well-known Bragg effect, their period scales with signal wavelength, and hence the dimensions of the structure might be too high (in certain applications) to achieve the desired rejection levels. And still others proposed high performance Hi-Lo microstrip low-pass filters with lumped elements [4], however, the use of lumped elements raises fabrication difficulties.

Recently, fractal-shaped coupled-line microstrip bandpass filters (BPFs) [5] and stepped-impedance transformers (SITs) [6] were proposed, because of the weak current discontinuities of the fractal-shaped geometry in the passband, the fractal-shaped BPFs and SITs achieved high performance. For this article, fractal-shaped Hi-Lo microstrip low-pass filters are proposed for the first time. It will be demonstrated that, with the use of the fractal-shaped geometry, the current discontinuities in the passband caused by high-low-steps are reduced greatly, and the resultant

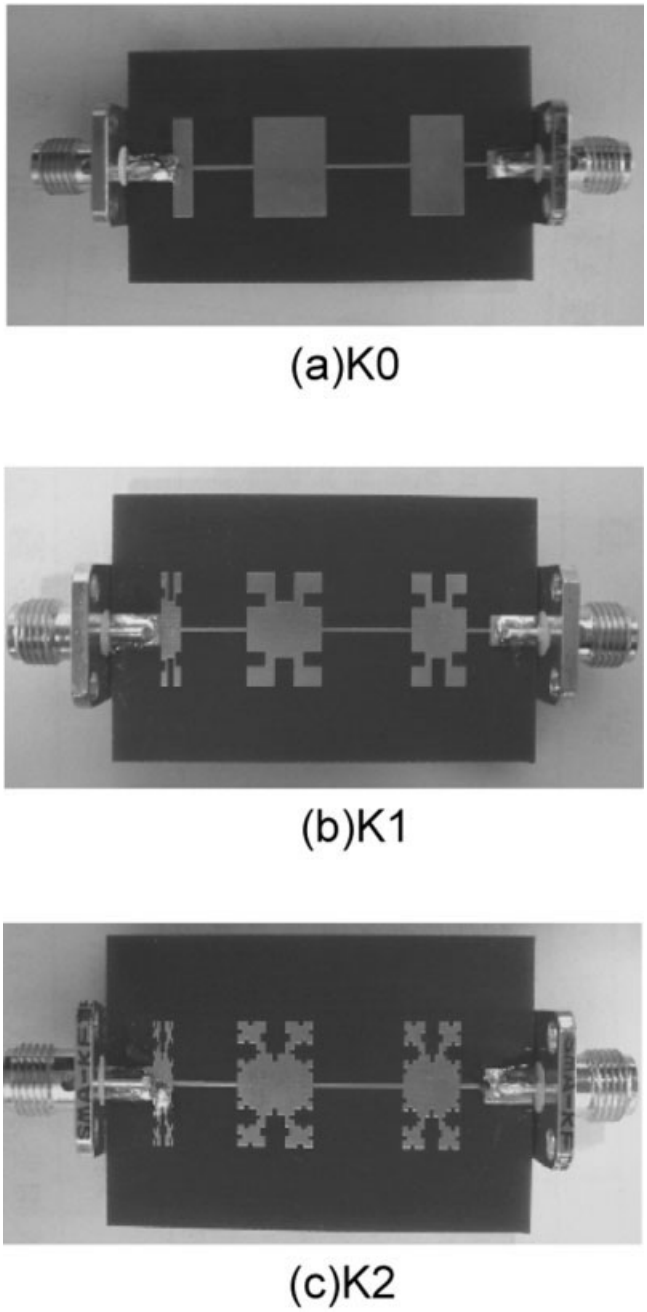

Figure 1 Prototypes of the fabricated fractal-shaped Hi-Lo microstrip LPFs. K0: zeroth iteration order, K1: first iteration order, K2: second iteration order